Predictive Analysis of the ITER Poloidal Field Conductor Insert (PFCI) Test Program

R. Zanino, M. Astrov, M. Bagnasco, W. Baker, F. Bellina, D. Ciazynski, S. Egorov, K. Kim, J. L. Kvitkovic, B. Lacroix, N. Martovetsky, N. Mitchell, L. Muzzi, Y. Nunoya, K. Okuno, M. Polak, P. L. Ribani, E. Salpietro, L. Savoldi Richard, C. Sborchia, Y. Takahashi, P. Weng, R. Wesche, L. Zani, and E. Zapretilina

***Abstract*—In this paper we discuss the predictive analysis performed in support of the test program of the International Thermonuclear Experimental Reactor (ITER) Poloidal Field Conductor Insert (PFCI). A subset of the test program items was considered, with particular emphasis on DC performance and AC losses. The results and implications of the comparison of selected predictions from different laboratories will be presented.**

***Index Terms*—Fusion reactors, ITER, modeling, superconducting magnets.**

I. Introduction

THE International Thermonuclear Experimental Reactor (ITER) is going to be built at Cadarache, France, over the next 10 years and it should then operate for another 20 years. So far, three superconducting insert coils (single-layer solenoids) were built and tested inside the bore of the ITER Central Solenoid Model Coil (CSMC), at JAEA Naka, Japan, in order to characterize the performance of selected conductors under ITER-relevant operating conditions. The ITER Poloidal Field Conductor Insert (PFCI) is presently under final acceptance at Tesla Engineering (UK). It will be the first insert coil based on NbTi [1], [2] and it is aimed at bridging the extrapolation gap between its full-size short (∼2–3 m long) sample, the PFCI-FSJS, which was tested in 2004 at the SULTAN facility in Switzerland [3], and the ITER PF coils, with particular relevance to the PF1 and PF6 (same cable layout but for the Cu-nonCu ratio), which among the PF coils are those at relatively higher field and, as such, the most critical.

The PFCI is a single-layer solenoid, wound from about 50 m of a full-size dual-channel ITER cable-in-conduit conductor, including an intermediate joint (IJ) located at relatively high magnetic field. It is cooled by supercritical helium at about 4.5 K and 0.6 MPa and carries a current of up to 45 (52) kA in normal (backup) mode, at 6 T peak external magnetic field. Details of the experimental set-up and sensor location have been given in [1]. The PFCI will be tested inside the bore of the ITER CSMC, which provides the background magnetic field.

The results of the PFCI-FSJS test were not completely satisfactory as, first, the joint resistance ($\sim 10\ \mathrm{n\Omega}$) was far above the ITER standards (1–2 $\mathrm{n\Omega}$) and, second, a significant reduction of the performances with respect to those of a single isolated strand was measured at high currents (i.e., above ∼25–30 kA), associated to a premature and sudden quench.

It is therefore essential, among other issues, to assess in a full-size, long NbTi conductor, to what extent the single-strand performances can be approached in a coil.

II. Test Program

The aim of the test and the corresponding main test program items have been already sketched in [1]. With respect to that, most of the detailed scenarios have now been defined [4].

In view of the above-mentioned shortcomings of the PFCI-FSJS test results, a major item in the PFCI test program is the DC characterization of the conductor, for which current sharing temperature ($\mathrm{T_{CS}}$) measurements will be performed, with a few critical current ($\mathrm{I_C}$) measurements to confirm the results. Considering the dramatic sensitivity of NbTi full-size conductors to the current distribution at high transport current [3], [5], several potentially mitigating mechanisms or conditions could in principle improve the coil performances with respect to those of the short sample, e.g.: 1) the joint/termination resistance improved thanks to the addition of SnPb solder [1], which might be accompanied by more uniform contacts between strand and copper sleeve; 2) the larger distance between joint/termination and peak field region, which gives the current distribution more room to diffuse; 3) the longer length at peak field, which could in principle help redistribution close to current sharing (although the relatively large inter-strand resistance makes this redistribution difficult [6], [7]). On the other hand, the magnetic field gradient on the cable cross section turns out to be comparable and large (∼1 T at 45 kA) in the two cases.

Manuscript received August 29, 2006. This work, supported by the European Communities under the contract of Association between EURATOM/ENEA, and by the Italian Ministry for Education, University and Research (MIUR), was carried out within the framework of the European Fusion Development Agreement. The views and opinions expressed herein do not necessarily reflect those of the European Commission.

R. Zanino, M. Bagnasco and L. S. Richard are with Dipartimento di Energetica, Politecnico, I-10129 Torino, Italy (e-mail: roberto.zanino@polito.it).

M. Astrov, S. Egorov and E. Zapretilina are with the Efremov Institute, St. Petersburg, Russia.

W. Baker and E. Salpietro are with EFDA Garching, Germany.

F. Bellina is with Universita' di Udine, Italy.

D. Ciazynski, B. Lacroix and L. Zani are with CEA Cadarache, France.

K. Kim is with NFRC, Daejeon, Korea.

J. L. Kvitkovic and M. Polak are with SAVBA, Bratislava, Slovakia.

N. Martovetsky is with LLNL, Livermore (CA) USA.

N. Mitchell and Y. Takahashi are with ITER IT, Naka, Japan.

L. Muzzi is with ENEA Frascati, Italy.

Y. Nunoya and K. Okuno are with JAEA Naka, Japan.

P. L. Ribani is with Universita' di Bologna, Italy.

C. Sborchia is with IPP Greifswald, Germany.

P. Weng is with CAS, Beijing, China.

R. Wesche is with EPFL-CRPP, Villigen, Switzerland.

Digital Object Identifier 10.1109/TASC.2007.899046

Another test program item, which recently received a lot of attention, is the study of the dependence of the AC losses on cycling electromagnetic load—10000 cycles being presently foreseen in the PFCI test program. Here the critical issue will be to determine if the losses (after an initial decrease) tend to increase again, as observed on both sub-size [6] and full-size [7] NbTi samples measured in the Twente press, or else they saturate at a relatively low level, as observed on sub-size samples measured in SULTAN [8], i. e., under (body) force conditions closer to actual operation than the (surface) load conditions of the press.

Finally, as a contribution to the assessment of the safety margin for the ITER PF coil operation in varying fields, a subset of the PFCI tests is planned using the JT-60 power supply, including the ramp-rate limitation (RRL) tests analysed below.

III. Predictive Analysis

Predictive simulations have been performed on the basis of the test program in the same flavor as for the PFCI-FSJS [9], but for a more comprehensive set of tests. Magnetic field maps and critical current scaling were taken from [1].

A. T_{CS}/I_C Tests

1) Scenario: Two $\mathrm{T_{CS}}$ tests have been chosen at $\mathrm{I_{PFCI}} = 18\ \mathrm{kA}$ and $\mathrm{I_{PFCI}} = 45\ \mathrm{kA}$, respectively. For both, $\mathrm{B} \sim 6\ \mathrm{T}(\mathrm{I_{CSMC}} \sim 21\ \mathrm{kA})$, $\mathrm{T_{in}(t = 0\ s)} = 4.5\ \mathrm{K}$, $\mathrm{p_{in}(t = 0)} = 0.6\ \mathrm{MPa}$, $\mathrm{dm/dt(t = 0)} = 10\ \mathrm{g/s}$ and $\mathrm{dT/dt} = 1\ \mathrm{mK/s}$.

2) Models and Results: Five different models have been applied: N. Martovetsky (NM) [10], the THELMA code [11], [12], R. Wesche (RW) [13], L. Zani (LZ) and E. Zapretilina (EZ) [9].

All of the models include i) the magnetic field gradient on the cable cross section, which is the single most important ingredient driving the transition of full-size NbTi CICC [3] and ii) the temperature gradient along the conductor. Different values of heat transfer coefficient between helium and strand $\mathrm{h_{StHe}}$ in the range 200–1000 $\mathrm{W/m^2\ K}$ have been considered, but do not appear to play a dramatic role.

Major differences among the models concern the description of a non uniform current distribution and the inclusion of temperature gradients (both solid and fluid components) on the cable cross section—both features being peculiar to the THELMA code. The THELMA code uses for this purpose a nested discretization of the cable cross section going down to the single strand level, with 18 cable elements (CE) and 7 fluid channels (6 petals + hole) in total [2]. A lower and an upper bound for current nonuniformity on the cable cross section have been considered: the current imposed at the cable boundaries in the most loaded strand (MLS), i.e., the CE corresponding to a single strand that experiences the highest magnetic field, has been varied from $\mathrm{I_{MLS}/I_{AVE}} = 1$ (resulting from the most optimistic assumption of uniform current distribution in the cable) to $\mathrm{I_{MLS}/I_{AVE}} = 3.6$ (most conservative assumption, supported by measurements of the joint contact resistances performed at CRPP [5]) and non-uniform current distribution in the other CEs as computed by THELMA [12]. Note however that, while the PFCI is equipped with Hall Probe heads to measure the current non-uniformity at the petal level, which is expected to be small, the current non-uniformity inside the petal and, even worse, down to the strand level, is presently not validated.

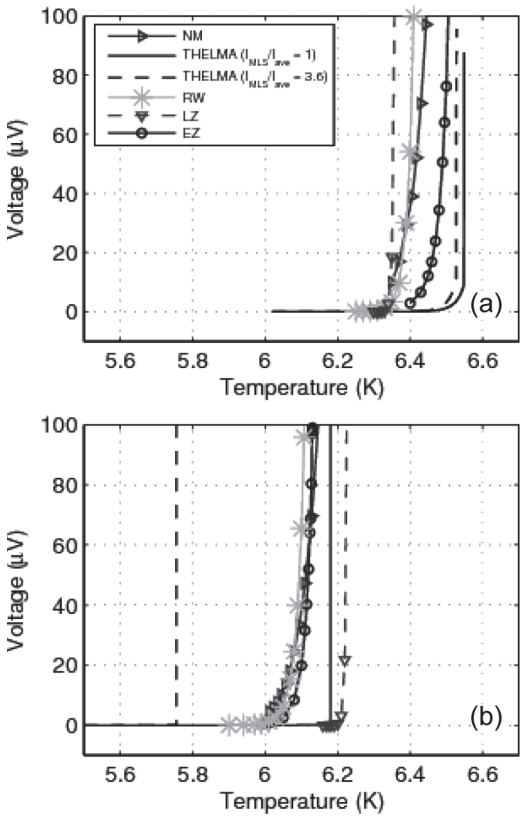

Fig. 1. Predicted voltage-temperature (V-T) characteristics at 18 kA (a) and 45 kA (b), based on different models. The abscissa represents the inlet helium temperature, the ordinates the total voltage on the main winding.

The computed voltage evolutions during the $\mathrm{T_{CS}}$ scenarios are presented in Fig. 1(a) and (b) for 18 kA and 45 kA, respectively, as a function of the inlet He temperature (equal to the temperature just downstream of the lower termination, if heat generation and transfer there are neglected).

At $\mathrm{I_{PFCI}} = 18\ \mathrm{kA}$, a smooth transition is computed by several predictors, see Fig. 1(a), with $\mathrm{T_{CS}}$ in the range 6.35–6.55 K. The practically sudden transitions predicted by LZ and (to some extent) THELMA, which run away before a measurable voltage is reached, could be due both to the large n value assumed (LZ) and/or to the overestimation of local effects (THELMA) already noted in the PFCI-FSJS analysis [12].

At $\mathrm{I_{PFCI}} = 45\ \mathrm{kA}$, the nature of the predicted transition depends even more on the model used, see Fig. 1(b). A sudden quench (whose mechanism was already discussed in [2]) is predicted by THELMA and LZ, but the quench temperature strongly depends on the assumption of current overload on the MLS (THELMA). Under the optimistic assumption of homogeneous current distribution, the predicted best performance foresees a sudden quench at ~6.2 K. The location of the initial normal zone can be influenced by the actual evolution of the inlet temperature in the experiment (ramp rates, temperature ripples). For the overload $\mathrm{I_{MLS}/I_{AVE}} = 3.6$, a *premature* sudden quench at ~5.7 K is computed by THELMA and this is the predicted worst coil performance. The relatively large

uncertainty in the prediction (∼0.4–0.5 K out of a total margin of ∼1.5 K) is a direct consequence of the above-mentioned sensitivity of NbTi full-size conductors to current distribution. On the contrary, at 18 kA the overload has almost no impact, because the field gradient on the cable cross section is proportionally smaller. A similar threshold for the transition is computed by RW, NM and EZ, but in their case the transition is smooth. This difference may be attributed to the fact that in THELMA (see above) the local Joule heating is not spread over the whole cable but contributes in the first place to the local temperature increase of the MLS. This drives the take-off of the peak electric field on the MLS, before any noticeable average electric field is present on the cable [2].

On the above-mentioned potentially mitigating mechanisms, compared to the short sample, we may add from the simulation that, in the PFCI, the longer distance between the lower termination and the peak field region allows indeed some diffusion of the current profile, reducing the MLS overload by typically ∼10–20% compared to the value imposed at the cable boundaries. On the other hand, as to the longer length at peak field, the present condition of temperature gradient along the conductor, combined with the high n and dE/dT values of NbTi, makes this mechanism rather inefficient for current redistribution.

B. AC Losses

1) Scenario: Two scenarios have been chosen:

- *Exponential discharge mode*: $\mathrm{I_{PFCI}} = 0\ \mathrm{kA}$, $\mathrm{I_{CSMC}(t = 0)} = 21.2\ \mathrm{kA}$; time constant $= 20\ \mathrm{s}$; $\mathrm{T_{in}} = 4.5\ \mathrm{K}$.
- *Trapezoidal mode*: $\mathrm{I_{PFCI}} = 0\ \mathrm{kA}$, $\mathrm{dB_{CSMC}/dt\ (up/down)} = \pm 0.5\ \mathrm{T/s}$; flat top $\mathrm{I_{CSMC}} = 21.2\ \mathrm{kA}$; $\mathrm{t_{flat\ top}} = 5\ \mathrm{s}$; $\mathrm{T_{in}} = 4.5\ \mathrm{K}$.

2) Losses in the Conductor: Models and Results: Three different models have been used for the AC loss computation: a similar approach by B. Lacroix (BL) and EZ, and the THELMA code. The analysis of BL is based on classical formulas for coupling and hysteretic losses in a cable, characterized by a time constant $\mathrm{n}\tau = 20\ \mathrm{ms}$ and by an effective diameter $\mathrm{d_{eff}} = 5\ \mu\mathrm{m}$, respectively, derived from short sample tests [3], [7]. EZ has developed a model which includes also the effect of cycling and load, mimicking the behavior of the cable apparent time constant $(\mathrm{n}\tau)$, which is known from previous experiments [7]. The approach to the modeling method was first described in [14]. The model simulates three main tendencies of $\mathrm{n}\tau$ behavior: its dependence of field rate, loading history and applied load. Also EZ accounts for hysteresis losses. On the other hand, the THELMA code computes the coupling losses directly from the simulated induced current loops in the conductor. The discretization of the cable cross section goes down to the last-but-*two* cable stage [15], i.e., the $3 \times 4 \times 4$ bundles, for a total of 30 CE. Intra- and inter-petal transverse conductances are taken from short sample measurements [7] at $\mathrm{N} = 0$ (virgin state) and $\mathrm{N} = 10000$ cycles. Hysteresis losses are not included in THELMA.

Results are presented in Fig. 2. In the exponential scenario [Fig. 2(a)], EZ predicts losses increasing with cycling, as the model is based on the short sample results [7]. While the initial magnitude of the losses along the whole conductor is comparable, the decay computed by BL is faster than that by EZ. This

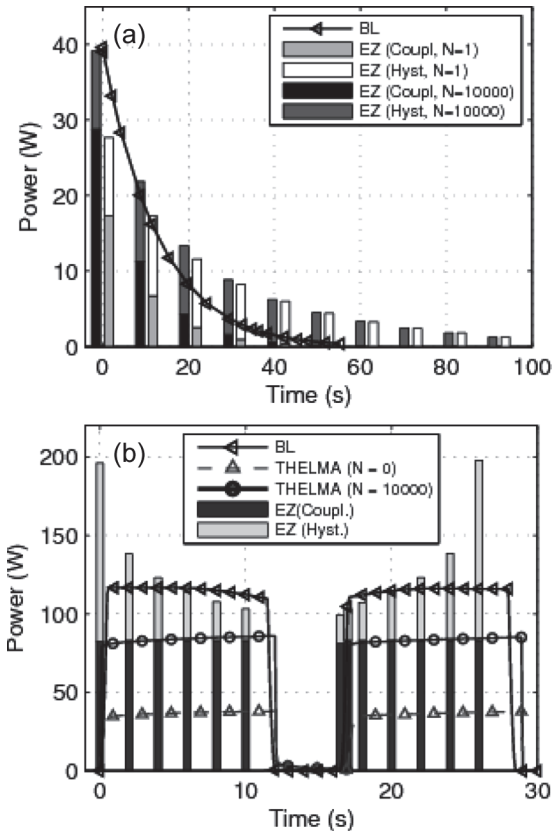

Fig. 2. Predicted evolution of the power deposited in the conductor as a function of time, for different scenarios: exponential (a) and trapezoidal (b), based on different models. In (a) the results of EZ are for two different numbers of cycles N, whereas in (b) $N = 10000$ is considered by EZ and two different N by THELMA.

could be attributed to the fact that, after a while, only hysteresis losses $(\propto \mathrm{J_C} \times \mathrm{dB/dt})$ survive and the prediction by EZ stays above BL who assumes a constant $\mathrm{J_C}$ for $\mathrm{B} < 2.5\ \mathrm{T}$.

In the trapezoidal scenario [Fig. 2(b)], EZ predicts at $\mathrm{N} = 10000$ the same coupling loss as THELMA. However, note that the THELMA result constitutes in principle a lower bound for the coupling losses estimate, because intra-bundle losses (inside the $3 \times 4 \times 4$ stage) are not included in the model. In the virgin state, THELMA predicts a lower loss than at $\mathrm{N} = 10000$, roughly proportional to the lower contact resistance between CEs measured in the short sample [7]. At low field (start and end of ramp), hysteresis losses are important, see also above, as confirmed by EZ predictions.

Using the computed AC losses as input, the temperature increase $\Delta\mathrm{T}$ at the main winding outlet, which will be the most relevant measurable quantity for the calorimetric assessment of the losses, has been computed: $\Delta\mathrm{T} < 0.1\ \mathrm{K}$ for the exponential discharge (BL, [16]) and $\Delta\mathrm{T} \sim 0.25/0.3\ \mathrm{K}$ for the trapezoidal pulse (BL/THELMA).

3) Losses in the Intermediate Joint: Models and Results: Results for the exponential discharge mode were already presented and discussed in [1]. Here we concentrate therefore on the trapezoidal scenario. The model of D. Ciazynski (DC) is described in [17]. In THELMA, the joint has been modeled considering the six petals as individual cable elements, magnetically coupled with each other and with the CSMC. The saddle and the sleeves

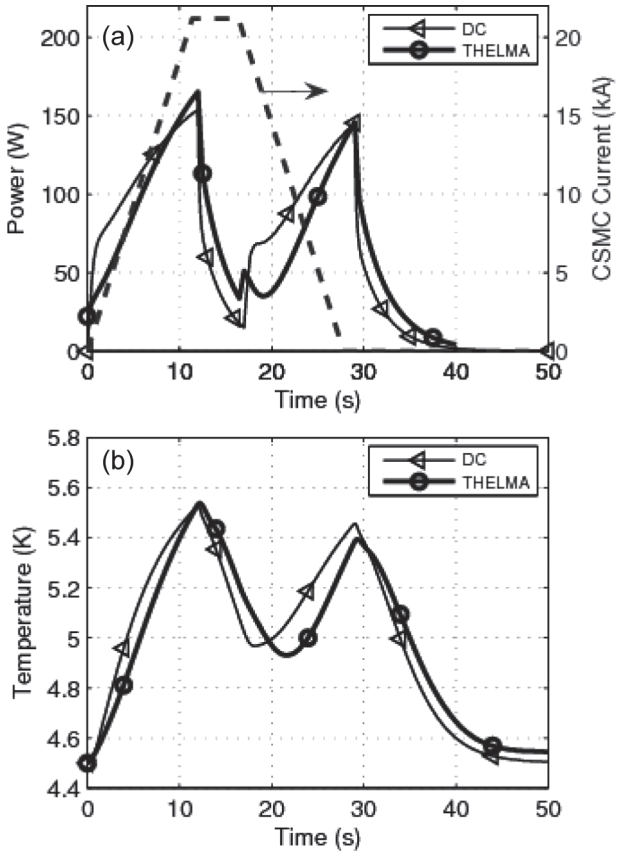

Fig. 3. Predicted power deposited in the IJ as a function of time, for the trapezoidal scenario, and corresponding temperature increase across the joint, based on different models (see text).

are modeled as resistive induced voltage generators, which depend on the CSMC current. Details of the THELMA joint model can be found in [18]. The results of the two models shown in Fig. 3 are very close. The maximum He ΔT across the joint resulting from the losses was computed with the Mithrandir code [19] and is not negligible ($\sim$1 K, computed neglecting conservatively the heat transfer to the colder busbar side). It represents at the same time a lower bound of the temperature jump on the busbar side, raising the issue of a possible quench of the joint/busbar in the RRL scenarios (see below), which will have higher ramp rates and nonzero current in the PFCI. On the contrary, this estimate seems to indicate that the joint losses should not be so important for the case of the ITER PF1,6 joints, based on present scenarios which have max dB/dt $\sim$0.25 T/s.

C. Quench Propagation

A quench will be initiated by the inductive heater. The scenario studied here is: $I_{PFCI} = 45$ kA, $I_{CSMC} = 21$ kA, $T_{in}(t = 0) = 5$ K, $dm/dt(t = 0) = 10$ g/s, $pin(t = 0) = 0.6$ MPa, 20 ms pulse. The simulation has been performed with the Mithrandir code, which, however, was validated so far only for quench propagation in Nb_3Sn conductor inserts with a similar setup [20], [21]. In order to account for the *local* nature of the sudden quench in NbTi, the conductor n-value has been set to a very large value. The boundary conditions are kept fixed, which usually leads to a slight overestimation of the quench speed. The whole conductor becomes normal in $\sim$6 s. In order to roughly account for the *premature* nature of the sudden quench, notwithstanding the uniform current assumption in Mithrandir, the temperature margin has been reduced by 0.4 K, see Fig. 1. In this case, the results show a much faster quench propagation—the whole conductor becomes normal in $\sim$3 s. In the two cases, the computed $T_{HOTSPOT}$ *before dump* is $\sim$60 K and $\sim$40 K, respectively.

TABLE I
SUMMARY OF RRL PREDICTIONS

dB/dt (T/s)	nτ (ms)	T_{max} (K)	B_{max} (T)	I_{max} (kA)
2	20	5.7	7.4	26.0
	40	6.3	6.3	22.1
	100	7.3	4.1	14.4

D. Ramp Rate Limitation (RRL)

RRL tests of the PFCI will have to be performed connecting it in series with the CSMC, implying rather limited flexibility. The most stringent scenario is defined by the following parameters: $dB/dt = 2\,T/s, T_{in}(t = 0\,s) = 4.5\,K, p_{in}(t = 0) = 0.6\,MPa$, $dm/dt(t = 0) = 10\,g/s$.

A single model (NM) was used for the predictions. It assumes a uniform current distribution and computes the losses as hysteresis losses in the filaments and coupling losses in the cable. Coupling losses in the strands are ignored, since they are included in the cable losses, which are taken from short sample experiments [7], parametrically varying $n\tau$ between 20 and 100 ms. The generated heat is then used to compute the temperature rise and to calculate the local I_C. When the transport current is equal to the local I_C, it is defined as the maximum achievable current I_{max}. The results of the analysis are shown in Table I. In view of the uniform current distribution assumption, they represent sort of upper bound estimates for the PFCI performance under these transient conditions.

REFERENCES

[1] R. Zanino *et al.*, "Preparation of the ITER Poloidal Field Conductor Insert (PFCI) test," *IEEE Trans. Appl. Supercond.*, vol. 15, pp. 1346–1350, 2005.
[2] R. Zanino *et al.*, "Implications of NbTi short-sample test results and analysis for the ITER Poloidal Field Conductor Insert (PFCI)," *IEEE Trans. Appl. Supercond.*, vol. 16, pp. 886–889, 2006.
[3] P. Bruzzone *et al.*, "Test results of the ITER PF insert conductor short sample in SULTAN," *IEEE Trans. Appl. Supercond.*, vol. 15, pp. 1351–1354, 2005.
[4] R. Zanino, "Status of PFCI test program," presented at the ITER Magnet Meeting on PFCI, Naka, Japan, May 22, 2006, unpublished.
[5] P. Bruzzone, "Status of technology tasks at CRPP," presented at the EU Magnet Experts Meeting, Barcelona, Spain, May 16, 2006, unpublished.
[6] Y. A. Ilyin, A. Nijhuis, W. Abbas, and H. H. J. ten Kate, "Electromagnetic performance of sub-size NbTi CICC's subjected to transverse cyclic loading," *IEEE Trans. Appl. Supercond.*, vol. 14, pp. 1503–1506, 2004.
[7] Y. A. Ilyin *et al.*, "Effect of cyclic loading and conductor layout on contact resistance of full-size ITER PFCI conductors," *IEEE Trans. Appl. Supercond.*, vol. 15, pp. 1359–1362, 2005.
[8] P. Bruzzone, B. Stepanov, and E. Zapretilina, "A critical review of coupling loss results for cable-in-conduit conductors," *IEEE Trans. Appl. Supercond.*, vol. 16, pp. 827–830, 2006.

[9] D. Ciazynski *et al.*, "DC performances of ITER NbTi conductors: Models vs. measurements," *IEEE Trans. Appl. Supercond.*, vol. 15, pp. 1355–1358, 2005.

[10] N. Martovetsky, "Stability and thermal equilibrium in cable-in-conduit conductors," *Physica C*, vol. 401, pp. 118–123, 2004.

[11] M. Ciotti, A. Nijhuis, P. L. Ribani, L. S. Richard, and R. Zanino, "THELMA code electromagnetic model of ITER superconducting cables and application to the ENEA stability experiment," *Supercond. Sci. Technol.*, vol. 19, pp. 987–997, 2006.

[12] M. Bagnasco, F. Bellina, P. L. Ribani, L. S. Richard, and R. Zanino, "Multi-solid multi-channel THELMA analysis of sudden quench of ITER superconducting NbTi full-size short samples," presented at the CHATS06, Berkeley, CA, USA, September 2006, unpublished.

[13] R. Wesche, A. Anghel, B. Stepanov, M. Vogel, and P. Bruzzone, "DC performance, AC loss and transient field stability of five medium size NbTi cable-in-conduit conductors with parametric variations," *Cryogenics*, vol. 45, pp. 755–779, 2005.

[14] R. Zanino, L. S. Richard, and E. Zapretilina, "Modeling of thermal-hydraulic effects of AC losses in the central solenoid insert coil using the M&M code," *IEEE Trans. Appl. Supercond.*, vol. 13, pp. 1424–1428, 2003.

[15] R. Zanino *et al.*, "Modeling AC losses in the ITER NbTi Poloidal Field Full Size Joint Sample (PF-FSJS) using the THELMA code," *Fus. Eng. Des.*, vol. 75–79C, pp. 23–27, 2005.

[16] L. Bottura, C. Rosso, and M. Breschi, "A general model for thermal, hydraulic and electric analysis of superconducting cables," *Cryogenics*, vol. 40, pp. 617–626, 2000.

[17] D. Ciazynski and A. Martinez, "Electrical and thermal designs and analyses of joints for the ITER PF coils," *IEEE Trans. Appl. Supercond.*, vol. 12, pp. 538–542, 2002.

[18] F. Bellina, "The THELMA model of the Poloidal Field Conductor (PFCI) Insert Joint," presented at the ASC, Seattle, WA, USA, September 2006, unpublished.

[19] R. Zanino, S. DePalo, and L. Bottura, "A two-fluid code for the thermohydraulic transient analysis of CICC superconducting magnets," *J. Fus. Energy*, vol. 14, pp. 25–40, 1995.

[20] L. Savoldi, E. Salpietro, and R. Zanino, "Inductively driven transients in the CS insert coil (II): Quench tests and analysis," *Adv. Cryo. Eng.*, vol. 47, pp. 423–430, 2002.

[21] L. S. Richard, A. Portone, and R. Zanino, "Tests and analysis of quench propagation in the ITER toroidal field conductor insert," *IEEE Trans. Appl. Supercond.*, vol. 13, pp. 1412–1415, 2003.